 MCB, vol.10, no.3, pp.201-232, 2013

Application of Different Variants of the BEM in Numerical Modeling of Bioheat Transfer Problems

Ewa Majchrzak*

Abstract: Heat transfer processes proceeding in the living organisms are described by the different mathematical models. In particular, the typical continuous model of bioheat transfer bases on the most popular Pennes equation, but the Cattaneo-Vernotte equation and the dual phase lag equation are also used. It should be pointed out that in parallel are also examined the vascular models, and then for the large blood vessels and tissue domain the energy equations are formulated separately.
In the paper the different variants of the boundary element method as a tool of numerical solution of bioheat transfer problems are discussed. For the steady state problems and the vascular models the classical BEM algorithm and also the multiple reciprocity BEM are presented. For the transient problems connected with the heating of tissue, the various tissue models are considered for which the 1^{st} scheme of the BEM, the BEM using discretization in time and the general BEM are applied.
Examples of computations illustrate the possibilities of practical applications of boundary element method in the scope of bioheat transfer problems.

Keywords: bioheat transfer models, Pennes equation, Cattaneo-Vernotte equation, dual-phase lag equation, boundary element method, heating of tissue

1 Introduction

Bioheat transfer models proposed in the literature can be divided into two categories, namely tissue models and vascular ones [1]. Currently, most of the existing models bases on the continuous Pennes equation [2]. Generally speaking, the Pennes equation corresponds to the well known Fourier equation supplemented by the additional components which take into account the global effect of the heat

* Institute of Computational Mechanics and Engineering, Silesian University of Technology, 44-100 Gliwice, Konarskiego 18a, Poland.
Email: ewa.majchrzak@polsl.pl

exchange between the blood vessels and the surrounding tissue. At present, it is said that the tissue properties (in particular its heterogeneity) cause that the better models can be formulated on the basis of Cattaneo-Vernotte equation [3, 4] and dual-phase lag equation [5, 6]. The assumption of the finite velocity of thermal wave causes a delay of heat flux in relation to the temperature gradient (Cattaneo-Vernotte equation) and additionally a delay of temperature gradient in relation to the heat flux (dual-phase lag equation).

Vascular models try to reproduce the real network of blood vessels in the tissues and describe the local changes in temperature within individual blood vessels. However, the more exact vascular models required the detailed knowledge of blood vessels geometry, the direction of blood flow, etc.

The influence of the external thermal effects is taken into account at the stage of the boundary conditions formulation. Heat exchange between the skin surface and the environment is determined by the processes of radiation, convection, evaporation (sweating) and the action of controlled or uncontrolled external heat sources.

In this study, the possibilities of the boundary element method (BEM) application for the numerical modelling of bioheat transfer problems are discussed [7, 8, 9].

So, for the steady state tasks the possibilities of the multiple reciprocity BEM applications are presented [10]. For the transient bioheat transfer problems described by the Pennes equation the 1^{st} scheme of the BEM [7, 9] and the BEM using discretization in time [7, 9, 11] are used, while to solve the Cattaneo-Vernotte equation or the dual-phase lag equation the generalized boundary element method [12, 13] is proposed.

Examples of calculations are mainly connected with the tissues models and they concern the computations of temperature distribution in the injured and healthy tissue (steady state problem) and the modelling of tissue heating (transient problem). The vascular models are also discussed, in particular the numerical solution concerning the thermal processes proceeding within a perfused tissue in the presence of the blood vessels (artery and vein) is shown.

2 Bioheat transfer equations

Bioheat transfer in biological tissue domain is usually described by the equation basing on the classical Fourier law

$$\mathbf{q}(x,\, t) = -\lambda \nabla T(x,\, t) \tag{1}$$

and then the energy equation takes a form

$$x \in \Omega: \quad c\frac{\partial T(x,t)}{\partial t} = -\nabla \mathbf{q}(x,t) + Q(x,t) \tag{2}$$

In equations (1) and (2) $\mathbf{q}$ denotes the heat flux, $\nabla T(x,t)$ is the temperature gradient, λ is the thermal conductivity of tissue, c is the volumetric specific heat of tissue, $Q(x, t)$ is the capacity of internal volumetric heat sources, x,t are the spatial co-ordinates and time.

Introducing (1) into (2) one obtains the traditional energy equation

$$x \in \Omega \; : \quad c\frac{\partial T(x,t)}{\partial t} = \lambda \nabla^2 T(x,t) + Q(x,t) \tag{3}$$

In the case of bioheat transfer the component $Q(x, t)$ (the Pennes approach) is the sum of perfusion and metabolic heat sources, in particular

$$Q(x,t) = G_B c_B [T_B - T(x,t)] + Q_m \tag{4}$$

where G_B is the blood perfusion coefficient, c_B is the volumetric specific heat of blood, T_B is the arterial temperature and Q_m is the metabolic heat source.

The modifications of equation (3) result from the acceptation of generalized forms of the Fourier law. For example, the Cattaneo-Vernotte model results from the formula

$$\mathbf{q}(x, t+\tau_q) = -\lambda \nabla T(x,t) \tag{5}$$

where $\tau_q = a/C^2$ is called the relaxation time, $a = \lambda/c$ is a thermal diffusivity and C is a speed of thermal wave in the medium.

The first order Taylor expansion of formula (5) gives

$$\mathbf{q}(x,t) + \tau_q \frac{\partial \mathbf{q}(x,t)}{\partial t} = -\lambda \nabla T(x,t) \tag{6}$$

Putting (6) into (2) one obtains the following modified bioheat transfer equation

$$x \in \Omega \; : \quad c\left[\frac{\partial T(x,t)}{\partial t} + \tau \frac{\partial^2 T(x,t)}{\partial t^2}\right] = \lambda \nabla^2 T(x,t) + Q(x,t) + \tau \frac{\partial Q(x,t)}{\partial t} \tag{7}$$

Heat transfer in biological tissues can be also described by dual-phase-lag model [5, 6] basing on the assumption that

$$\mathbf{q}(x, t+\tau_q) = -\lambda \nabla T(x, t+\tau_T) \tag{8}$$

where τ_T is the thermalization time, it is the phase-lag in establishing the temperature gradient across the medium during which conduction occurs through its small-scale structures [5].

Taking into account the first order Taylor expansions for $\mathbf{q}$ and T

$$q(x,t)+\tau_q\frac{\partial\,\mathbf{q}(x,t)}{\partial\,t}=-\lambda\nabla T(x,t)-\lambda\,\tau_T\frac{\partial\,\nabla T(x,t)}{\partial\,t} \tag{9}$$

one obtains the following dual-phase-lag equation

$$\begin{aligned} x\in\Omega\ :\ c\left[\frac{\partial\,T(x,t)}{\partial\,t}+\tau_q\frac{\partial^2 T(x,t)}{\partial\,t^2}\right]=\\ \lambda\nabla^2 T(x,t)+\lambda\,\tau_T\frac{\partial\,\nabla^2 T(x,t)}{\partial\,t}+Q(x,t)+\tau_q\frac{\partial\,Q(x,t)}{\partial\,t} \end{aligned} \tag{10}$$

In the case of steady state conditions, the equations above presented give the well known Poisson one

$$\lambda\nabla^2 T(x)+Q(x)=0 \tag{11}$$

3 Boundary element method for steady state bioheat transfer equation

The Pennes equation for the steady state problem can be written in the form (c.f. equations (3), (11))

$$\lambda\nabla^2 T(x)+G_B\,c_B\,[T_B-T(x)]+Q_m=0 \tag{12}$$

or

$$\lambda\nabla^2 T\,(x)-G_B\,c_B\,T\,(x)+Q=0 \tag{13}$$

where $Q=G_B\,c_B\,T_B+Q_m$.

To solve the equation (13) the multiple reciprocity boundary element method (MRBEM) [10, 14] has been applied. This variant of the BEM allows one to avoid the discretization of domain interior. So, the following integral equation is considered [14]

$$\begin{aligned} B(\xi)T(\xi)+\sum_{l=0}^{\infty}\left(\tfrac{G_B\,c_B}{\lambda}\right)^l\int_\Gamma q(x)V_l^*(\xi,x)\,\mathrm{d}\Gamma=\\ \sum_{l=0}^{\infty}\left(\tfrac{G_B\,c_B}{\lambda}\right)^l\int_\Gamma T(x)Z_l^*(\xi,x)\,\mathrm{d}\Gamma-\tfrac{Q}{\lambda}\sum_{l=1}^{\infty}\left(\tfrac{G_B\,c_B}{\lambda}\right)^{l-1}\int_\Gamma Z_l^*(\xi,x)\,\mathrm{d}\Gamma \end{aligned} \tag{14}$$

where ξ is the observation point, $q(x)$= -λ n•$\nabla T(x)$ is the boundary heat flux (n is the normal outward vector). The coefficient $B(\xi)$ is dependent on the location of source point ξ. For all points located inside the domain Ω the coefficient $B(\xi)$ =1. If the point ξ belongs to the boundary Γ this coefficient is equal to $\beta/2\pi$, where β

is an internal angle which the boundary makes at the point ξ. Thus, for a smooth boundary the value $B(\xi)$ =0.5 is obtained.

Functions $V_l^*(\xi,x)$ for 2D and 3D problems are defined as follows [10, 14]

$$V_l^*(\xi,x) = \begin{cases} \frac{1}{2\pi\lambda} r^{2l}\left(A_l \ln\frac{1}{r} + B_l\right) & \text{for 2D problem} \\ \frac{1}{4\pi\lambda} r^{2l-1} C_l & \text{for 3D problem} \end{cases} \tag{15}$$

where r is the distance between the points ξ and x, while

$$\begin{array}{llll} A_0 = 1, & & A_l = \frac{A_{l-1}}{4l^2}, & l = 1,2,3,... \\ B_0 = 0, & B_l = \frac{1}{4l^2}\left(\frac{A_{l-1}}{l} + B_{l-1}\right), & & l = 1,2,3,... \end{array} \tag{16}$$

and

$$C_0 = 1, \quad C_1 = \frac{1}{2}, \quad C_2 = \frac{1}{24}, \quad C_l = \frac{1}{(2l-1)(2l-3)} C_{l-1}, \quad l = 3,4,5,... \quad . \tag{17}$$

The heat fluxes $Z_l^*(\xi, x) = -\lambda\, \mathrm{n}\cdot\nabla V_l^*(\xi, x)$ resulting from the fundamental solutions (15) can be calculated analytically and then

$$Z_l^*(\xi,x) = \begin{cases} \frac{d}{2\pi} r^{2l-2}\left[A_l - 2l\left(A_l \ln\frac{1}{r} + B_l\right)\right] & \text{for 2D problem} \\ -\frac{d}{4\pi}(2l-1)\, r^{2l-3} C_l & \text{for 3D problem} \end{cases} . \tag{18}$$

where

$$d = \sum_{e=1}^{w} (x_e - \xi_e)\cos\alpha_e \tag{19}$$

while $\cos\alpha_e$ are the directional cosines of the normal boundary vector and w is the problem dimension.

The other variants of the boundary element method can be also considered, for example fast multipole BEM [15] or dual reciprocity BEM [16].

It should be pointed out that in the case when, for example, burned tissue or bone tissue is considered the blood perfusion and metabolic heat source do not occur and then G_B=0 and Q_m=0 (c.f. equation (13)). Then, the Pennes equation reduces to the Laplace one for which the boundary integral equation has the following form

$$B(\xi)T(\xi) + \int_\Gamma q(x) V_0^*(\xi,x)\,\mathrm{d}\Gamma = \int_\Gamma T(x) Z_0^*(\xi,x)\,\mathrm{d}\Gamma \tag{20}$$

4 Boundary element method for transient bioheat transfer equations

From the mathematical point of view the Pennes equation (4) is the parabolic one, the Cattaneo-Vernotte equation (7) is the hyperbolic one, while the DPL equation (10) contains a second order time derivative and higher order mixed derivative in both time and space.

To solve the Pennes equation by means of the boundary element method the several variants basing on a time marching technique can be applied, this means the 1^{st} scheme of the BEM e.g. [17, 18, 19], the BEM using discretization in time e.g. [20] and the dual reciprocity BEM [21, 22, 23]. The other approaches can be also developed (e.g. [24]).

At first, the time grid should be introduced

$$0 = t^0 < t^1 < ... < t^{f-2} < t^{f-1} < t^f < ... < t^F < \infty \tag{21}$$

with the constant time step $\Delta t = t^f - t^{f-1}$.

In the case of 1^{st} *scheme of the BEM* for transition $t^{f-1} \rightarrow t^f$ the following boundary integral equation corresponding to the Pennes equation (4) is considered [7, 9] (c.f. equation (23)

$$\begin{aligned} &B(\xi)T(\xi,t^f) + \frac{1}{c}\int_{t^{f-1}}^{t^f}\int_{\Gamma} T^*(\xi,x,t^f,t)q(x,t)d\Gamma dt = \\ &\frac{1}{c}\int_{t^{f-1}}^{t^f}\int_{\Gamma} q^*(\xi,x,t^f,t)T(x,t)d\Gamma dt + \int_{\Omega} T^*(\xi,x,t^f,t^{f-1})T(x,t^{f-1})d\Omega + \\ &\frac{1}{c}\int_{t^{f-1}}^{t^f}\int_{\Omega} Q(x,t^f)T^*(\xi,x,t^f,t)d\Omega dt \end{aligned} \tag{22}$$

where $T^*(\xi, x, t^f, t)$ is the fundamental solution and it is a function of the form

$$T^*(\xi,x,t^f,t) = \frac{1}{[4\pi a(t^f-t)]^{w/2}} \exp\left[-\frac{r^2}{4a(t^f-t)}\right] \tag{23}$$

while ξ denotes a source point, r is the distance between the points x and ξ, w is the problem dimension, $a = \lambda/c$ is the diffusion coefficient and $q(x,t)$= - λ n•$\nabla T(x,t)$.

The heat flux resulting from fundamental solution should be found using the formula $q^*(\xi, x, t^f, t)$ = - λ n•$\nabla T^*(\xi, x, t^f, t)$ and after mathematical manipulations one obtains

$$q^*(\xi,x,t^f,t) = \frac{\lambda d}{2\cdot 2^w \pi^{\frac{w}{2}} [a(t^f-t)]^{\frac{w+2}{2}}} \exp\left[-\frac{r^2}{4a(t^f-t)}\right] \tag{24}$$

where d is defined by the dependency (19).

Another approach related to the Pennes equation solution is to replace the derivative with respect to time by differential quotient. This variant of the BEM is called *the BEM using discretization in time* [7, 9, 11]. Thus, taking into account the formula (3), the Pennes equation (3) can be written in the form

$$c\frac{\partial T(x,t)}{\partial t} = \lambda \nabla^2 T(x,t) - G_B c_B T(x,t) + Q \tag{25}$$

where, as previously, $Q = G_B c_B T_B + Q_m$.

For time $t \in [t^{f-1}, t^f]$ the following approximate form of the equation (25) is considered

$$\frac{T(x,t^f) - T(x,t^{f-1})}{\Delta t} = a\nabla^2 T(x,t^f) - \frac{G_B c_B}{c} T(x,t^f) + \frac{Q}{c} \tag{26}$$

and then

$$\nabla^2 T(x,t^f) - AT(x,t^f) + \tfrac{1}{a\Delta t} T(x,t^{f-1}) + \tfrac{Q}{\lambda} = 0 \tag{27}$$

where $A=(c + G_B c_B \Delta t)/(\lambda \Delta t)$.

This approach is close to the finite difference method in the case of transient thermal diffusion problems. Using the weighted residual criterion [7, 9] one obtains the following boundary integral equation

$$\begin{aligned} &B(\xi)T(\xi,t^f) + \tfrac{1}{\lambda}\int_\Gamma T^*(\xi,x)q(x,t^f)d\Gamma = \tfrac{1}{\lambda}\int_\Gamma q^*(\xi,x)T(x,t^f)d\Gamma + \\ &\tfrac{1}{a\Delta t}\int_\Omega T(x,t^{f-1})T^*(\xi,x)d\Omega + \tfrac{Q}{\lambda}\int_\Omega T^*(\xi,x)d\Omega \end{aligned} \tag{28}$$

where $T^*(\xi, x)$ is the fundamental solution and for the objects oriented in rectangular co-ordinate system it is a function of the form

$$T^*(\xi,x) = \begin{cases} \frac{1}{2\sqrt{A}} \exp\left(-r\sqrt{A}\right), & \text{for 1D problem} \\ \frac{1}{2\pi} K_0\left(r\sqrt{A}\right), & \text{for 2D problem} \\ \frac{1}{4\pi r} \exp\left(-r\sqrt{A}\right), & \text{for 3D problem} \end{cases} \tag{29}$$

where $K_0(\cdot)$ is the modified Bessel function of zero order [7, 9].

Heat flux resulting from the fundamental solution can be found using the formula $q^*(\xi, x) = -\lambda\, n \bullet \nabla T^*(\xi, x)$

$$q^*(\xi,x) = \begin{cases} \frac{\lambda sgn(x-\xi)}{2} \exp\left(-r\sqrt{A}\right), & \text{for 1D problem} \\ \frac{\lambda d}{2\pi r} K_1\left(r\sqrt{A}\right), & \text{for 2D problem} \\ \frac{\lambda d}{4\pi r^2} \exp\left(-r\sqrt{A}\right)\left(\frac{1}{r} + \sqrt{A}\right), & \text{for 3D problem} \end{cases} \tag{30}$$

where $K_1(\cdot)$ is the modified Bessel function of the second kind of order one [7, 9] and sgn(•) is the sign function.

It should be pointed out that in order to improve the exactness of this variant of the BEM the following approximation of equation (25) for $t \in [t^{f-2}, t^f]$ can be taken into account

$$\frac{3\,T(x,t^f)-4T(x,t^{f-1})+T(x,t^{f-2})}{2\Delta t}=a\nabla^2\,T(x,t^f)-\frac{G_B c_B}{c}T(x,\,t^f)+\frac{Q}{c} \tag{31}$$

The details of this approach can be found, among others, in [7].

In the case of Cattaneo-Vernotte equation or dual-phase-lag equation the boundary element method is more complicated because the corresponding fundamental solution is either unknown or very difficult to obtain. A natural way to solve these equations is to apply the concept of generalized variant of the BEM using discretization in time.

Because for τ_T =0 the dual-phase-lag equation reduces to the Cattaneo-Vernotte equation, therefore the algorithm for the first of these equations will be presented here.

Taking into account the form (3) of source function the dual-phase-lag equation (10) can be written as follows

$$\begin{aligned} &c\left[\frac{\partial\,T(x,t)}{\partial\,t}+\tau_q\frac{\partial^2 T(x,t)}{\partial\,t^2}\right]=\lambda\nabla^2 T(x,t)+\lambda\,\tau_T\frac{\partial\,\nabla^2 T(x,t)}{\partial\,t}- \\ &G_B c_B T(x,t)+Q-G_B c_B\tau_q\frac{\partial\,T(x,t)}{\partial\,t} \end{aligned} \tag{32}$$

Approximate form of equation (32) results from the introduction of differential quotients, in particular

$$\begin{aligned} &c\left[\frac{T(x,t^f)-T(x,t^{f-1})}{\Delta t}+\tau_q\frac{T(x,t^f)-2T(x,t^{f-1})+T(x,t^{f-2})}{(\Delta t)^{\,2}}\right]= \\ &\lambda\nabla^2 T(x,t^f)+\frac{\lambda\,\tau_T}{\Delta t}\left[\nabla^2 T(x,t^f)-\nabla^2 T(x,t^{f-1})\right]-G_B c_B T(x,t^f)+ \\ &Q-G_B c_B\tau_q\frac{T(x,t^f)-T(x,t^{f-1})}{\Delta t} \end{aligned} \tag{33}$$

or

$$\nabla^2\,T(x,\,t^f)-AT(x,\,t^f)+R\left[T(x,t^{f-1})\right]=0 \tag{34}$$

where

$$A=\frac{(\Delta t+\tau_q)(c+G_B c_B\Delta t)}{\lambda\,\Delta t(\Delta t+\tau_T)} \tag{35}$$

and

$$R\left[T(x,t^{f-1})\right] = -\frac{\tau_T}{\Delta t+\tau_T}\nabla^2 T(x,t^{f-1}) + \frac{c\,(\Delta t+2\tau_q)+G_B c_B\,\tau_q\,\Delta t}{\lambda\,\Delta t\,(\Delta t+\tau_T)}T(x,t^{f-1}) - \frac{c\,\tau_q}{\lambda\,\Delta t\,(\Delta t+\tau_T)}T(x,t^{f-2}) + \frac{Q\,\Delta t}{\lambda\,(\Delta t+\tau_T)} \tag{36}$$

Using the weighted residual criterion [7, 9] one obtains the following boundary integral equation

$$B(\xi)T(\xi,t^f) + \frac{1}{\lambda}\int_\Gamma T^*(\xi,x)q(x,t^f)d\Gamma = \frac{1}{\lambda}\int_\Gamma q^*(\xi,x)T(x,t^f)d\Gamma + \int_\Omega R\left[T(x,t^{f-1})\right]T^*(\xi,x)d\Omega \tag{37}$$

where fundamental solution $T^*(\xi, x)$ is described by formula (29), while the function $q^*(\xi, x)$ by formula (30).

However, numerical experiments show that this variant of the BEM gives inaccurate results, especially in the case of the dual-phase-lag equation.

The effective tool to solve the dual-phase-lag equation is the *generalized boundary element method* (GBEM) [12, 13]. From the mathematical point the of view the theoretical bases of GBEM are rather complicated, but at the stage of numerical algorithm construction the procedures are similar to other variants of the BEM. At the beginning, the derivatives with respect to time in the dual-phase-lag equation (32) are replaced by the differential quotients and then the equation (34) is obtained. Next, for the successive transitions $t^{f-1} \to t^f$ the following equation must be solved

$$\nabla^2 U^{[1]}(x) - AU^{[1]}(x) + R\left[T(x,t^{f-1})\right] = 0 \tag{38}$$

where

$$U^{[1]}(x) = \left.\frac{\partial\,\Phi(x;p)}{\partial\,p}\right|_{p=0} \tag{39}$$

while $\Phi(x; p)$ is called homotopy [12], p is the embedding parameter.

The boundary integral equation corresponding to equation (38) has the following form

$$B(\xi)U^{[1]}(\xi) + \tfrac{1}{\lambda}\int_\Gamma T^*(\xi,x)\,W^{[1]}(x)d\Gamma = \tfrac{1}{\lambda}\int_\Gamma q^*(\xi,x)\,U^{[1]}(x)d\Gamma + \int_\Omega R\,[T(x,t^{f-1})]\,T^*(\xi,x)d\Omega \tag{40}$$

where$W^{[1]}(x)$= -λ n•$\nabla U^{[1]}(x)$ and the functions $T^*(\xi, x)$, $q^*(\xi, x)$ are described by formulas (29), (30), respectively.

After solving (40), the temperature $T(x, t^f)$ is determined from the equation

$$T(x, t^f) = T(x, t^{f-1}) + U^{[1]}(x) \tag{41}$$

or [25]

$$T_k(x, t^f) = T_{k-1}(x, t^{f-1}) + mU^{[1]}(x), \quad k = 1, 2, ..., K \tag{42}$$

where $T_0(x,t^f) = T(x,t^{f-1})$, m is an iterative parameter and K is the number of iterations.

Examples of computations - steady state problems

The first example concerns the computations of temperature field in the non-homogeneous domain being the composition of burned and healthy tissue [26, 27]. The steady state Pennes equation for healthy tissue is of the form

$$x \in \Omega_2 : \quad \lambda_2 \nabla^2 T_2(x) + G_B c_B [T_B - T_2(x)] + Q_m = 0 \tag{43}$$

where T_2 (x) is the tissue temperature, λ_2 is the tissue thermal conductivity, G_B is the blood perfusion coefficient, c_B is the volumetric specific heat of blood, T_B is the arterial blood temperature, Q_m is the metabolic heat source, x are the spatial co-ordinates, x=$\{x_1, x_2\}$ for 2D problem, x=$\{x_1, x_2, x_3\}$ for 3D problem.

For the burned tissue, blood perfusion and metabolic heat generation are equal to zero, because the tissue is dead. So

$$x \in \Omega_1 : \quad \lambda_1 \nabla^2 T_1(x) = 0 \tag{44}$$

where λ_1 is the thermal conductivity of burned tissue.

On the surface between sub-domains the continuity of heat flux and temperature field is assumed

$$x \in \Gamma_c : \quad \begin{cases} -\lambda_1 n \cdot \nabla T_1(x) = -\lambda_2 n \cdot \nabla T_2(x) \\ T_1(x) = T_2(x) \end{cases} \tag{45}$$

On the skin surface (Figure 1) being in a thermal contact with an environment the Robin condition should be taken into account

$$x \in \Gamma_{ex} : \quad -\lambda_1 n \cdot \nabla T_1(x) = \alpha [T_1(x) - T_a], \quad e = 1, 2 \tag{46}$$

where α is the heat transfer coefficient, T_a is the ambient temperature.

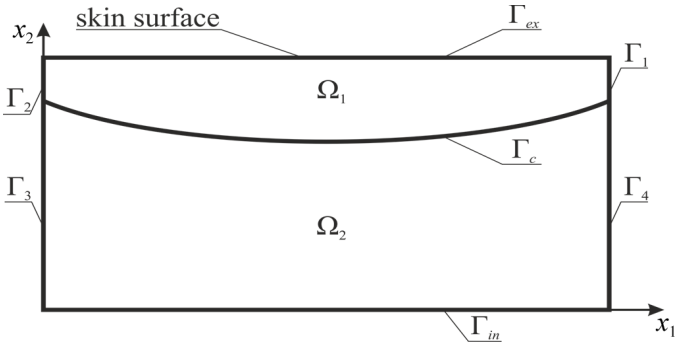

Figure 1: Domain considered

At the internal surface the body core temperature is known

$$x \in \Gamma_{in}: \qquad T_2(x) = T_b \tag{47}$$

For the others boundaries the no-flux conditions can be assumed.

The problem has been solved by coupling of the multiple reciprocity BEM for healthy tissue (equation (14)) and classical algorithm of the BEM for burned tissue (equation (20)).

To solve the equations (20) and (14) the boundary Γ is divided into N elements Γ_j =1,2,...,N. Then

$$B(\xi)\,T_1(\xi) + \sum_{j=1}^{N_1} \int_{\Gamma_j} q_1(x)\,V_0^*(\xi,\,x)\,d\Gamma_j = \sum_{j=1}^{N_1} \int_{\Gamma_j} T_1(x)\,Z_0^*(\xi,\,x)\,d\Gamma_j \tag{48}$$

and

$$\begin{aligned} &B(\xi)T_2(\xi) + \sum_{l=0}^{\infty} \left(\frac{G_B c_B}{\lambda_2}\right)^l \sum_{j=N_1+1}^{N} \int_{\Gamma_j} q_2(x) V_l^*(\xi,x)\,d\Gamma_j = \\ &\sum_{l=0}^{\infty} \left(\frac{G_B c_B}{\lambda_2}\right)^l \sum_{j=N_1+1}^{N} \int_{\Gamma_j} T_2(x) Z_l^*(\xi,x)\,d\Gamma_j - \frac{Q}{\lambda_2} \sum_{l=1}^{\infty} \left(\frac{G_B c_B}{\lambda_2}\right)^{l-1} \sum_{j=N_1+1}^{N} \int_{\Gamma_j} Z_l^*(\xi,x)\,d\Gamma_j \end{aligned} \tag{49}$$

where N_1 is the number of elements resulting from the discretization of the boundary limiting domain Ω_1.

It should be pointed out that different types of boundary elements can be used, namely constant elements, linear or parabolic ones [7, 9]. Here the linear boundary elements are applied as shown in Figure 2.

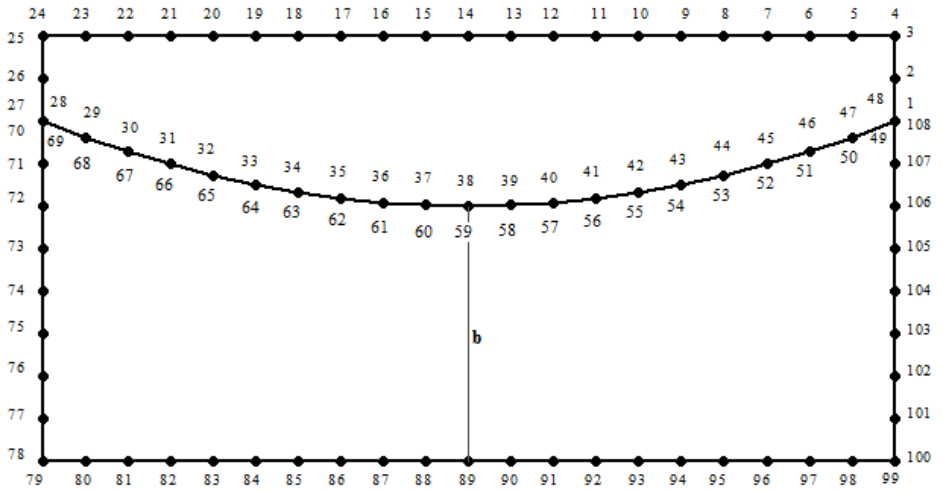

Figure 2: Discretization of boundaries

After the mathematical manipulations one obtains the following system of algebraic equations corresponding to the burned tissue [7, 9]

$$\sum_{k=1}^{K_1} G_{ik}^1 q_k^1 = \sum_{k=1}^{K_1} H_{ik}^1 T_k^1, \;\; k = 1,2,...,K_1 \tag{50}$$

and the system of equations corresponding to the healthy tissue

$$\sum_{k=K_1+1}^{K} G_{ik}^2 q_k^2 = \sum_{k=K_1+1}^{K_1} H_{ik}^2 T_k^2 + P_i, \;\; i = K_1+1, K_1+2, ...K \tag{51}$$

where K_1 is the number of boundary nodes located on the boundary limiting sub-domain Ω_1, $K - K_1$ is the number of boundary nodes located on the boundary limiting sub-domain Ω_2. For example, for 2D problem presented in Figure 2: K_1 =48, K =108. It should be pointed out that taking into account the form of boundary conditions, on the contact surface between sub-domains Ω_1 and Ω_2 (nodes 28-69 in Figure 2) the double boundary nodes should be introduced. The remaining double nodes (shown in Figure 2) for example 3-4, 24-25 correspond to different boundary conditions, namely nodes 4, 24 are connected with the Robin condition, while nodes 3, 25 are connected with the Neumann condition.

The system of algebraic equations corresponding to the equation (50) can be written in the form

$$\mathbf{G}_1 \mathbf{q}_1 = \mathbf{H}_1 \mathbf{T}_1 \tag{52}$$

and

$$\mathbf{G}_2\mathbf{q}_2 = \mathbf{H}_2\mathbf{T}_2 + \mathbf{P} \tag{53}$$

The way of matrix $\mathbf{G}_1, \mathbf{H}_1, \mathbf{G}_2, \mathbf{H}_2, \mathbf{P}$ elements computations is described in details in [7, 14].

For the needs of further considerations concerning the temperature field modeling the following denotations are introduced (c.f. Figures 1 and 2)

- $\mathbf{T}_1^1$, $\mathbf{T}_1^2$, $\mathbf{T}_1^{ex}$, $\mathbf{q}_1^1$, $\mathbf{q}_1^2$, $\mathbf{q}_1^{ex}$ are the vectors of functions T and q at the boundary $\Gamma_1 \cup \Gamma_2 \cup \Gamma_{ex}$ of domain Ω_1,
- $\mathbf{T}_{c1}$, $\mathbf{T}_{c2}$, $\mathbf{q}_{c1}$, $\mathbf{q}_{c2}$ are the vectors of functions T and q on the contact surface Γ_c between sub-domains Ω_1 and Ω_2,
- $\mathbf{T}_2^3$, $\mathbf{T}_2^4$, $\mathbf{T}_2^{in}$, $\mathbf{q}_2^3$, $\mathbf{q}_2^4$, $\mathbf{q}_2^{in}$ are the vectors of functions T and q at the boundary $\Gamma_3 \cup \Gamma_4 \cup \Gamma_{in}$ of domain Ω_2.

Using above designations one obtains the following systems of equations

- for the burned region

$$\begin{bmatrix} \mathbf{G}_1^1 & \mathbf{G}_1^{ex} & \mathbf{G}_1^2 & \mathbf{G}_{c1} \end{bmatrix} \begin{bmatrix} \mathbf{q}_1^1 \\ \mathbf{q}_1^{ex} \\ \mathbf{q}_1^2 \\ \mathbf{q}_{c1} \end{bmatrix} = \begin{bmatrix} \mathbf{H}_1^1 & \mathbf{H}_1^{ex} & \mathbf{H}_1^2 & \mathbf{H}_{c1} \end{bmatrix} \begin{bmatrix} \mathbf{T}_1^1 \\ \mathbf{T}_1^{ex} \\ \mathbf{T}_1^2 \\ \mathbf{T}_{c1} \end{bmatrix} \tag{54}$$

- for the healthy tissue domain

$$\begin{bmatrix} \mathbf{G}_{c2} & \mathbf{G}_2^3 & \mathbf{G}_2^{in} & \mathbf{G}_2^4 \end{bmatrix} \begin{bmatrix} \mathbf{q}_{c2} \\ \mathbf{q}_2^3 \\ \mathbf{q}_2^{in} \\ \mathbf{q}_2^4 \end{bmatrix} = \begin{bmatrix} \mathbf{H}_{c2} & \mathbf{H}_2^3 & \mathbf{H}_2^{in} & \mathbf{H}_2^4 \end{bmatrix} \begin{bmatrix} \mathbf{T}_{c2} \\ \mathbf{T}_2^3 \\ \mathbf{T}_2^{in} \\ \mathbf{T}_2^4 \end{bmatrix} + P \tag{55}$$

The condition (45) written in the form

$$\begin{cases} \mathbf{q}_{c1} = -\mathbf{q}_{c2} = \mathbf{q} \\ \mathbf{T}_{c1} = \mathbf{T}_{c2} = \mathbf{T} \end{cases} \tag{56}$$

should be introduced to the equations (54), (55). Next, coupling these systems of equations one has

$$\begin{bmatrix} \mathbf{G}_1^1 & \mathbf{G}_1^{ex} & \mathbf{G}_1^2 & -\mathbf{H}_{c1} & \mathbf{G}_{c1} & \mathbf{0} & \mathbf{0} & \mathbf{0} \\ \mathbf{0} & \mathbf{0} & \mathbf{0} & -\mathbf{H}_{c2} & -\mathbf{G}_{c2} & \mathbf{G}_2^3 & \mathbf{G}_2^{in} & \mathbf{G}_2^4 \end{bmatrix} \begin{bmatrix} \mathbf{q}_1^1 \\ \mathbf{q}_1^{ex} \\ \mathbf{q}_1^2 \\ \mathbf{T} \\ \mathbf{q} \\ \mathbf{q}_2^3 \\ \mathbf{q}_2^{in} \\ \mathbf{q}_2^4 \end{bmatrix} =$$

$$\begin{bmatrix} \mathbf{H}_1^1 & \mathbf{H}_1^{ex} & \mathbf{H}_1^2 & 0 & 0 & 0 \\ 0 & 0 & 0 & \mathbf{H}_2^3 & \mathbf{H}_2^{in} & \mathbf{H}_2^4 \end{bmatrix} \begin{bmatrix} \mathbf{T}_1^1 \\ \mathbf{T}_1^{ex} \\ \mathbf{T}_1^2 \\ \mathbf{T}_2^3 \\ \mathbf{T}_2^{in} \\ \mathbf{T}_2^4 \end{bmatrix} \tag{57}$$

The remaining boundary conditions should be also taken into account and then

$$\begin{bmatrix} -\mathbf{H}_1^1 & \alpha\mathbf{G}_1^{ex} - \mathbf{H}_1^{ex} & -\mathbf{H}_1^2 & -\mathbf{H}_{c1} & \mathbf{G}_{c1} & 0 & 0 & 0 \\ 0 & 0 & 0 & -\mathbf{H}_{c2} & -\mathbf{G}_{c2} & -\mathbf{H}_2^3 & \mathbf{G}_2^{in} & -\mathbf{H}_2^4 \end{bmatrix} \begin{bmatrix} \mathbf{T}_1^1 \\ \mathbf{T}_1^{ex} \\ \mathbf{T}_1^2 \\ \mathbf{T} \\ \mathbf{q} \\ \mathbf{T}_2^3 \\ \mathbf{q}_2^{in} \\ \mathbf{T}_2^4 \end{bmatrix} = \begin{bmatrix} \alpha\mathbf{G}_1^{ex}\mathbf{T}_a \\ \mathbf{G}_2^{in}\mathbf{T}_b \end{bmatrix} \tag{58}$$

As an example, the domain of dimensions 0.04m$\times$ 0.02m has been considered. The following input data have been assumed [26]: thermal conductivity of burned tissue λ_1=0.1 [W/(mK)], thermal conductivity of healthy tissue λ_2=0.2 [W/(mK)], blood perfusion coefficient G_B=0.0005 [1/s], volumetric specific heat of blood c_B=4.452 [MJ/(m^{3}K)], arterial blood temperature T_B=37^{o}C, metabolic heat source Q_m =200 [W/m^3], heat transfer coefficient α=10[W/ (m^{2}K)], ambient temperature T_a=20^{o}C. In Figure 3 the temperature distributions on the skin surface for different values of parabolic vertex b (c.f. Figure 2) this means 0.012 m, 0.014 m and 0.016 m are shown. The last curve corresponds to the constant burn depth, of course.

It should be pointed out that from the practical point of view this type of information is very important. The skin surface temperature is dependent on the local depth of

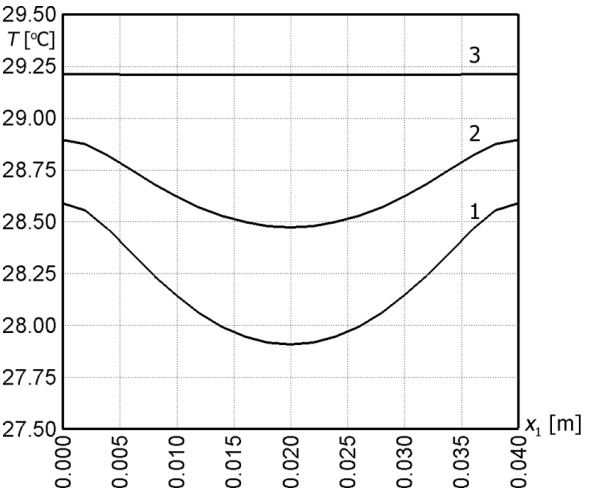

Figure 3: Temperature distribution at the skin surface: 1– b=0.012m, 2 – b=0.014 m, 3 – b=0.016 m.

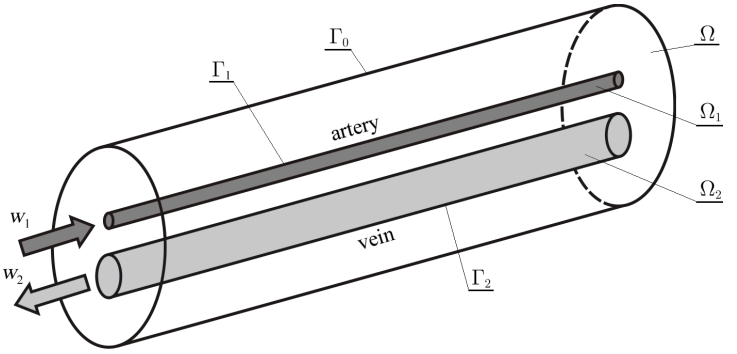

Figure 4: Pair of blood vessels

the burn wound. Thus, it is possible to estimate the shape of wound using, for example, the thermograms and solving the geometrical inverse problem [28].

As a second example, the thermal processes proceeding within a perfused tissue in the presence of the blood vessels (artery and vein) are analyzed. The domain considered corresponds to the so-called *Krogh-type tissue cylinder* [29] as shown in Figure 4, which is heated only by a pair of blood vessels located at a central part of cylinder, on the side surface the no-flux conditions can be assumed.

A steady state temperature field in tissue sub-domain is described by the Pennes equation (c.f. equation (12))

$$(x_1,x_2,z)\in\Omega:\quad \lambda\nabla^2 T\,(x_1,x_2,z)+G_B\,c_B\,[T_B-T\,(x_1,x_2,z)]+Q_m=0 \tag{59}$$

The boundary conditions on the contact surfaces between tissue and vessels are of the form of Robin ones

$$\begin{aligned}&(x_1,\,x_2,\,z)\in\Gamma_1:\quad q\,(x_1,\,x_2,\,z)=-\lambda\,\mathbf{n}\cdot\nabla T\,(x_1,\,x_2,\,z)=\alpha_1\,[T\,(x_1,\,x_2,\,z)-T_{B1}\,(z)]\\&(x_1,\,x_2,\,z)\in\Gamma_2:\quad q\,(x_1,\,x_2,\,z)=-\lambda\,\mathbf{n}\cdot\nabla T\,(x_1,\,x_2,\,z)=\alpha_2\,[T\,(x_1,\,x_2,\,z)-T_{B2}\,(z)]\end{aligned} \tag{60}$$

where $T_{B1}(z)$, $T_{B2}(z)$ are the blood temperatures inside artery and vein, respectively, α_1 and α_2 are the heat transfer coefficients. According to the literature [1, 29], under the assumption that the Nusselt number in the case considered equals to Nu = 4, one can determine directly the values of above coefficients.

As was mentioned, the boundary condition on the external surface of the system is of the form

$$(x_1,\,x_2,\,z)\in\Gamma_1:\quad q\,(x_1,\,x_2,\,z)=-\lambda\,\mathbf{n}\cdot\nabla T\,(x_1,\,x_2,\,z)=0 \tag{61}$$

Assuming that the changes of blood temperature are only the functions of co-ordinate z, and taking into account the countercurrent blood flow, one can write the following ordinary differential equations resulting from the energy balances [30]

$$(x_1,x_2,z)\in\Omega_1:\quad \frac{dT_{B1}\,(z)}{d\,z}=A_1\,[T_{v1}\,(z)-T_{B1}\,(z)]+B_1 \tag{62}$$

and

$$(x_1,x_2,z)\in\Omega_2:\quad \frac{dT_{B2}\,(z)}{d\,z}=-A_2\,[T_{v2}\,(z)-T_{B2}\,(z)]-B_2 \tag{63}$$

where

$$A_e=\frac{2\alpha_e}{w_e c_B R_e},\quad B_e=\frac{Q_{Bm}}{w_e c_B},\quad e=1,\,2 \tag{64}$$

while R_1, R_2 are the vessels radiuses, w_1, w_2 denote the blood rates inside artery and vein, Q_{Bm} is the metabolic heat source in blood vessels, while $T_{v1}(z)$, $T_{v2}(z)$ are the mean temperatures of vessels walls corresponding to the cross section z. On the basis of the Peclet number (Pe = 100 [1, 29]), one can determine the rates w_1 and w_2. The last equations are supplemented by the initial conditions, this means $T_{B1}(0) = T_{B10}$ and $T_{B2}(Z) = T_{B20}$, where Z is the length of the segment considered.

The problem has been solved using the iterative algorithm being the combination of the multiple reciprocity BEM (tissue) and the finite difference method (vessels). At first, the fixed section perpendicular to the vessels is considered as shown in Figure 5.

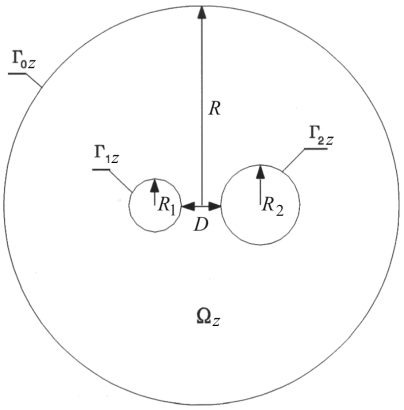

Figure 5: Section perpendicular to the vessels

For the cross section z the following equation (c.f. equation (59))

$$x \in \Omega_z : \quad \lambda \nabla^2 T(x) - G_B c_B T(x) + Q = 0\,, \quad x = \{x_1, x_2\} \tag{65}$$

supplemented by the boundary conditions (c.f. equations (60), (61))

$$\begin{aligned} x \in \Gamma_{1z} : &\quad q(x) = -\lambda\, \mathbf{n} \cdot \nabla T(x) = \alpha_1 \left[T_{v1}(z) - T_{B1}(z)\right] \\ x \in \Gamma_{2z} : &\quad q(x) = -\lambda\, \mathbf{n} \cdot \nabla T(x) = \alpha_2 \left[T_{v2}(z) - T_{B2}(z)\right] \\ x \in \Gamma_{0z} : &\quad q(x) = -\lambda\, \mathbf{n} \cdot \nabla T(x) = 0 \end{aligned} \tag{66}$$

is taken into account.

Application of multiple reciprocity boundary element method leads to the integral equation (14). To solve this equation the discretization of the boundary should be done (as shown in Figure 6) and the integrals in equation (14) are substituted by the

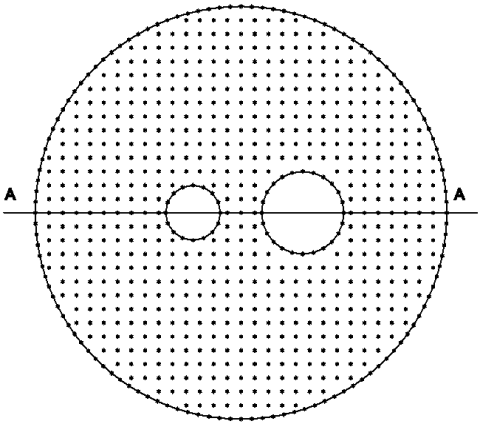

Figure 6: Discretization of the boundaries and internal nodes

sums of integrals over these elements. Parabolic boundary elements are used here and finally one obtains the following system of equations [31]

$$\sum_{k=1}^{K} G_{ik} q_k = \sum_{k=1}^{K} H_{ik} T_k + \sum_{k=1}^{K} P_{ik}, \quad i = 1,2,...,K \tag{67}$$

If one assumes that K_1 nodes are located at the boundaryΓ_{1z}, K_2 - K_1nodes are located at the boundary Γ_{2z} and the remaining nodes $K - K_2$ - K_1 are located at the boundaryΓ_{0z} then

$$\begin{aligned} &\sum_{k=1}^{K_1} G_{ik} q_k + \sum_{k=K_1+1}^{K_2} G_{ik} q_k + \sum_{k=K_2+1}^{K} G_{ik} q_k = \\ &\sum_{k=1}^{K_1} H_{ik} T_k + \sum_{k=K_1+1}^{K_2} H_{ik} T_k + \sum_{k=K_2+1}^{K} H_{ik} T_k + \sum_{k=1}^{K} P_{ik} \end{aligned} \tag{68}$$

Taking into account the boundary conditions (66), in the well-ordered form, one has

$$\begin{aligned} &\sum_{k=1}^{K_1} (\alpha_1 G_{ik} - H_{ik}) T_k + \sum_{k=K_1+1}^{K_2} (\alpha_2 G_{ik} - H_{ik}) T_k - \sum_{k=K_2+1}^{K} H_{ik} T_k = \\ &\sum_{k=1}^{K_1} \alpha_1 G_{ik} T_{B1}(z) + \sum_{k=K_1+1}^{K_2} \alpha_2 G_{ik} T_{B2}(z) + \sum_{k=1}^{K} P_{ik} \end{aligned} \tag{69}$$

It is visible, that the solution of this system of equations is possible under the assumption that the temperatures T_{B1}(z) and $T_{B2}(z)$ are known, and then the temperatures at the boundary nodes can be determined.

Next, the following approximation of equations (62), (63) is proposed

$$\frac{T_{B1}(z+\Delta z)-T_{B1}(z)}{\Delta z} = A_1 \left[T_{v1}(z) - T_{B1}(z)\right] + B_1 \tag{70}$$

and

$$\frac{T_{B2}(z+\Delta z)-T_{B2}(z)}{\Delta z} = -A_2 \left[T_{v2}(z) - T_{B2}(z)\right] - B_2 \tag{71}$$

So

$$T_{B1}(z+\Delta z) = (1 - A_1 \Delta z)\ T_{B1}(z) + A_1 \Delta z T_{v1}(z) + B_1 \Delta z \tag{72}$$

and

$$T_{B2}(z+\Delta z) = (1 + A_2 \Delta z)\ T_{B2}(z) - A_2 \Delta z T_{v2}(z) - B_2 \Delta z \tag{73}$$

The idea of the algorithm discussed is the following. For the cross section $z = 0$ and arbitrary assumed temperature $T_{B2}(0)$ (the temperature $T_{B1}(0) = T_{B10}$ is known from the initial condition, of course) the system of equations (69) is solved. Next, the mean values of vessels walls temperatures are calculated

$$T_{v1}(z) = \frac{1}{K_1} \sum_{k=1}^{K_1} T_k, \qquad T_{v2}(z) = \frac{1}{(K_2 - K_1)} \sum_{k=K_1+1}^{K_2} T_k \tag{74}$$

Putting $z = 0$ in equations (72) and (73) the temperatures $T_{B1}(\Delta z)$ and $T_{B2}(\Delta z)$ are calculated and these values are introduced to the system of equations (69). From this system of equations the boundary temperatures for cross section $z = \Delta z$ are determined. The mean values of vessels walls temperatures are determined from (74), next using the formulas (72), (73) the blood temperatures $T_{B1}(2\Delta z)$ and $T_{B2}(2\Delta z)$ can be found. These temperatures introduced to the system of equations (66) allow ones to calculate the boundary temperatures for the cross section $2\Delta z$. The procedure is continued until the cross section $z = Z$ is achieved. If $T_{B2}(Z) \neq T_{B20}$ then the procedure is repeated for the other value of $T_{B2}(0)$. The iteration process is continued until the calculated value $T_{B2}(Z)$ is close to the temperature T_{B20}

As an example, the following input data are assumed [31]: radius of artery R_1 = 0.0002 [m], radius of vein R_2 = 0.0003 [m], radius of Krogh-type tissue cylinder R= 0.0015 [m], distance between blood vessels D = 0.0003 [m] (Figure 5), length of cylinder Z = 0.06 [m], thermal conductivity of tissue λ = 0.5 [W/(mK)]. The inlet arterial blood temperature is set as $T_{B10} = T_B$ = 37.5°C, the inlet venous blood temperature T_{B20} = 37°C, perfusion coefficient equals to G_B = 0.0005425 [1/s], metabolic heat sources in tissue and vessels are Q_m = 245 [W/m^3] and Q_{Bm} = 100 [W/m^3], respectively. It is assumed that for the artery and vein Nu = 4, Pe = 100

and then the values of heat transfer coefficients correspond to $\alpha_1 = 5000$ [W/(m^{2}K)], $\alpha_2 = 3333.33$ [W/(m^{2}K)], while the blood rates are equal to $w_1 = 0.03$ [m/s] and $w_2 = 0.02$ [m/s].

The computations have been done under the assumption that the boundary of cross section (Figure 6) is divided into 80 parabolic boundary elements with $K = 160$ boundary nodes ($K_1 = 16$, $K_2 - K_1 = 24$ corresponds to the number of nodes located at the artery and vein walls, respectively) and $\Delta z = 2R_1$. Inside the tissue subdomain 620 internal nodes have been distinguished (see: Figure 6).

In Figures 7, 8, 9, 10 and 11 the results obtained are presented. In particular, the temperature distributions in the tissue domain for cross sections $z = 0$, 0.01, 0.02, 0.03 [m] are shown and the changes of blood temperature along artery-vein axes are presented. The calculated temperature of the venous blood leaving the tissue region equals to $T_{B2}(0) = 37.3^{\circ}$C. In Figure 12 the temperature distributions along the segments corresponding to plane of symmetry A-A (Figure 6) for diffrent values of co-ordinate z are shown.

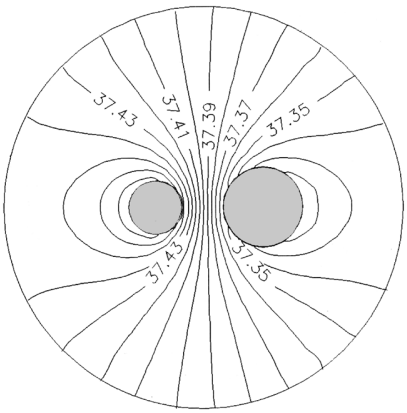

Figure 7: Temperature distribution ($z = 0$ m)

The example presented above is rather an academic one, because not all parameters can be found in the literature, but such models should be developed since they well describe the heat conduction especially in the extremities [32].

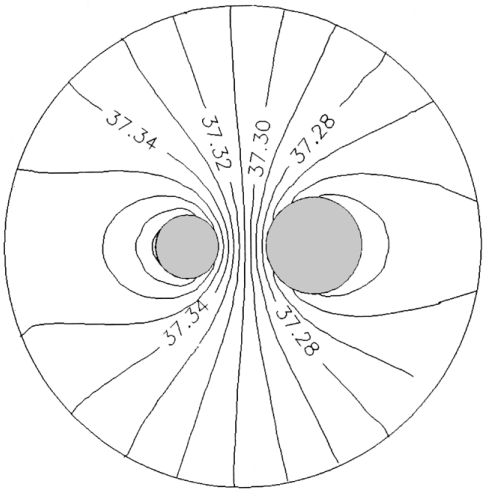

Figure 8: Temperature distribution ($z = 0.01$ m)

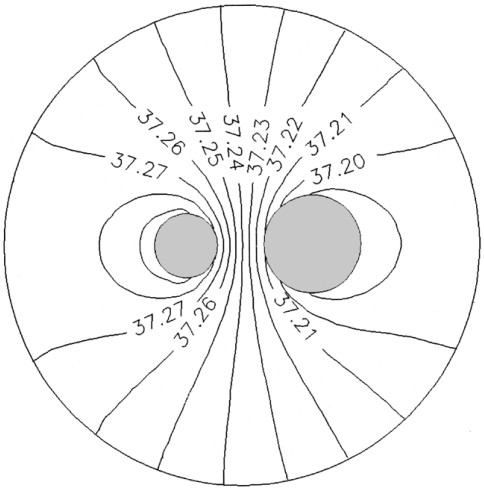

Figure 9: Temperature distribution ($z = 0.02$ m)

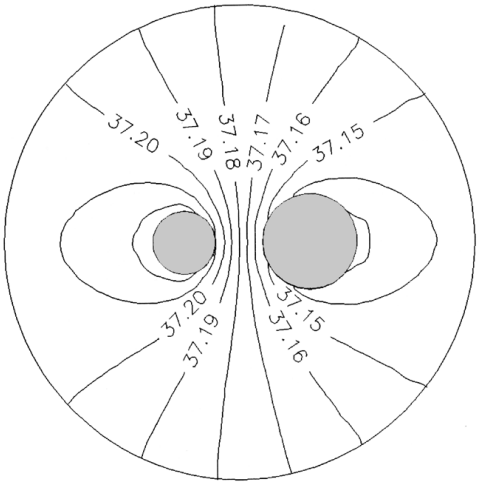

Figure 10: Temperature distribution ($z = 0.03$ m)

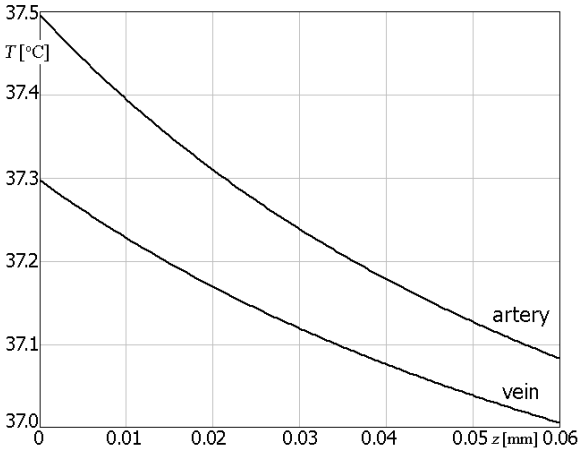

Figure 11: Temperature distribution along artery-vein axes

5 Examples of computations - transient problems

Biological tissue domain of dimensions $D \times D$ (square) shown in Figure 13 is considered. The upper surface is heated by the boundary heat flux in the form

$$x \in \Gamma_2 : \quad q_b(x,t) = q_b(x_1,D,t) = q_0 \frac{t}{t_e}\left(1-\frac{t}{t_e}\right)\exp\left(-\frac{x_1^2}{d^2}\right) \tag{75}$$

where q_0 is the maximum heat flux, t_e is the exposure time and $d = L/2$.

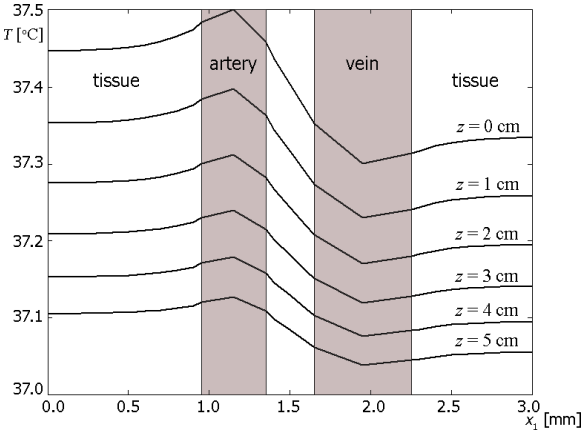

Figure 12: Temperature distribution along the sector A-A

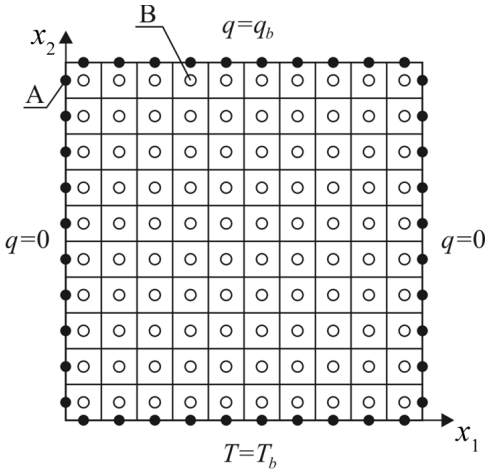

Figure 13: Boundary conditions and discretization

Along the boundary Γ_1 ($0 \leq x_1 \leq D$, x_2=0) the Dirichlet condition $T = T_b$ is assumed, on the remaining boundaries (Γ_3) the no-flux condition is taken into account. Initial temperature T_p of tissue is also given.

To determine the temperature distribution in the domain under consideration, the different models have been applied, namely the Pennes equation (4), the Cattaneo-Vernotte equation (7) and the dual-phase-lag equation (10).

In the case of Pennes model the 1^{st} scheme of the BEM has been used and then the boundary integral equation (22) should be solved. For the constant elements with

respect to time one obtains

$$B(\xi)T(\xi,t^f)+\int\limits_{\Gamma} q(x,t^f)g(\xi,x)d\Gamma=\int\limits_{\Gamma} T(x,t^f)h(\xi,x)d\Gamma+ \int\limits_{\Omega} T^*(\xi,x,t^f,t^{f-1})T(x,t^{f-1})d\Omega+\int\limits_{\Omega} Q(x,t^f)g(\xi,x)d\Omega \tag{76}$$

where

$$g(\xi,x)=\frac{1}{c}\int\limits_{t^{f-1}}^{t^f} T^*(\xi,x,t^f,t)dt \tag{77}$$

and

$$h(\xi,x)=\frac{1}{c}\int\limits_{t^{f-1}}^{t^f} q^*(\xi,x,t^f,t)dt \tag{78}$$

It should be pointed out that the integrals (77), (78) can be calculated in the analytical way [7, 29].

The integration with respect to the boundary Γ and interior Ω requires the introduction of geometrical mesh. So, the boundary Γ is divided into N boundary elements Γ_j, j=1, ..., N, while the interior Ω into L internal cells Ω_l, l=1, 2, ..., L.

If one assumes the constant boundary elements and constant internal cells then the formula (76) leads to the following system of algebraic equations (i=1, 2, ..., N)

$$\sum_{j=1}^{N} G_{ij}\,q_j^f=\sum_{j=1}^{N} H_{ij}\,T_j^f+\sum_{l=1}^{L} P_{il}\,T_l^{f-1}+\sum_{l=1}^{L} Z_{il}\,Q_l^f \tag{79}$$

where

$$G_{ij}=\int\limits_{\Gamma_j} g(\overset{\xi}{i},x)d\Gamma_j \tag{80}$$

$$H_{ij}=\begin{cases}\int\limits_{\Gamma_j} h(\xi_i,x)d\Gamma_j, i\neq j\\ -0.5, i=j\end{cases} \tag{81}$$

$$P_{il}=\int\limits_{\Omega_l} T^*(\xi_i,x,t^f,t^{f-1})d\Omega_l \tag{82}$$

$$Z_{il}=\int\limits_{\Omega_l} g(\xi_i,x)d\Omega_l \tag{83}$$

The matrix notation of the system (79) is the following

$$\mathbf{Gq}^f=\mathbf{HT}^f+\mathbf{PT}^{f-1}+\mathbf{ZQ}^f \tag{84}$$

Equation (84) allows one to determine the 'missing' boundary values (temperatures or heat fluxes) for time t^f.

In the second stage of algorithm the temperatures at internal nodesξ_i for $i = N+1$, $N+2$, ..., $N+L$ are calculated on the basis of formula

$$T_i^f = \sum_{j=1}^{N} H_{ij} T_j^f - \sum_{j=1}^{N} G_{ij} q_j^f + \sum_{l=1}^{L} P_{il} T_l^{f-1} + \sum_{l=1}^{L} Z_{il} Q_l^f \tag{85}$$

The temperature field obtained for time t^f constitutes the new pseudo-initial condition for the next step of computations.

To solve the Cattaneo-Vernotte equation and dual-phase-lag equation the generalized boundary element method has been applied. Because for τ_T=0 the dual-phase-lag equation reduces to the Cattaneo-Vernotte one therefore only the algorithm for DPL model (10) is discussed. This equation is supplemented by the boundary conditions

$$\begin{aligned} &x \in \Gamma_1: \quad T(x,t) = T_b \\ &x \in \Gamma_2: \quad q_b(x,t) + \tau_q \tfrac{\partial q_b(x,t)}{\partial t} = -\lambda \left[n \cdot \nabla T(x,t) + \tau_T \tfrac{\partial}{\partial t} \left(n \cdot \nabla T(x,t) \right) \right] \\ &x \in \Gamma_3: \quad 0 = -\lambda \left[n \cdot \nabla T(x,t) + \tau_T \tfrac{\partial}{\partial t} \left(n \cdot \nabla T(x,t) \right) \right] \end{aligned} \tag{86}$$

and initial ones

$$t = 0: \quad T(x,t) = T_p, \quad \left. \frac{\partial T(x,t)}{\partial t} \right|_{t=0} = 0 \tag{87}$$

where $q_b(x,t)$ is given by the formula (75).

Using generalized variant of the BEM, for transition $t^{f-1} \rightarrow t^f$ ($f \geq 2$) the following equation (c.f. equation (38)) is considered

$$\nabla^2 U^{[1]}(x) - B U^{[1]}(x) + R\left[T_{k-1}(x, t^{f-1}) \right] = 0 \tag{88}$$

with corresponding boundary conditions [13]

$$\begin{aligned} &x \in \Gamma_1: \quad U^{[1]}(x) = 0 \\ &x \in \Gamma_2: \quad W^{[1]}(x) = \tfrac{\Delta t}{\Delta t + \tau_T} \left[q_b(x, t^f) + \tau_q \left. \tfrac{\partial q_b(x,t)}{\partial t} \right|_{t=t^f} \right] \\ &\qquad -\tfrac{\lambda \tau_T}{\Delta t + \tau_T} n \cdot \nabla T(x, t^{f-1}) + \lambda\, n \cdot \nabla T_{k-1}(x, t^{f-1}) \\ &x \in \Gamma_3: \quad W^{[1]}(x) = -\tfrac{\lambda \tau_T}{\Delta t + \tau_T} n \cdot \nabla T(x, t^{f-1}) + \lambda\, n \cdot \nabla T_{k-1}(x, t^{f-1}) \end{aligned} \tag{89}$$

Comparing the equations (38) and (88) one can see that, according to the formula (42), the temperature $T(x, t^{f-1})$ is replaced by $T_{k-1}(x, t^{f-1})$.

As previously, the constant boundary elements and the constant internal cells are used and then one obtains the following approximation of equation (88)

$$\sum_{j=1}^{N} G_{ij} W_j^{[1]} = \sum_{j=1}^{N} H_{ij} U_j^{[1]} + \sum_{l=1}^{L} P_{il} R\left[T_{k-1}(x_l, t^{f-1})\right] \tag{90}$$

where

$$G_{ij} = \frac{1}{\lambda} \int_{\Gamma_j} T^*(\xi_i, x) d\Gamma_j \tag{91}$$

and

$$H_{ij} = \begin{cases} \int_{\Gamma_j} q^*(\xi_i, x) d\Gamma_j, & i \neq j \\ -0.5, & i = j \end{cases} \tag{92}$$

while

$$P_{il} = \int_{\Omega_l} T^*(\xi_i, x)\, d\,\Omega_l \tag{93}$$

Introducing the boundary conditions (89) into the linear algebraic equations (90) one obtains the equations for the unknown $W^{[1]}$ on the boundary Γ_1 and unknown $U^{[1]}$ on the boundaries Γ_2 and Γ_3. After solving the system of equations (90), the values $U^{[1]}$ at the internal points ξ_i are calculated using the formula

$$U_i^{[1]} = \sum_{j=1}^{N} H_{ij} U_j^{[1]} - \sum_{j=1}^{N} G_{ij} W_j^{[1]} + \sum_{l=1}^{L} P_{il} R\left[T_{k-1}(x_l, t^{f-1})\right] \tag{94}$$

Finally, for the all boundary and internal points the temperature values are determined on the basis of equation (42).

At the stage of computations the following input data have been assumed: the side of the square D=0.02 [m], the maximum heat flux q_0=25 [kW/m^2], the exposure time t_e=20 [s] (c.f. equation (75)), volumetric specific heat of tissue c =3 [MW/(m^{3}K)], thermal conductivity of tissue λ=0.5[W/(mK)], blood perfusion coefficient G_B=0.002 [1/s], volumetric specific heat of blood c_B=3.9962 [MW/(m^{3}K)], blood temperature T_B=37^{o}C, metabolic heat source Q_m=245 [W/m^3], relaxation time τ_q=15[s], thermalization time τ_T=10[s]. Initial temperature of tissue equals to T_p=37^{o}C.

The discretization of boundary and interior of the domain considered is shown in Figure 13. Calculations were performed under the assumption that the time step is

equal to Δt=1 [s] and the iterative parameter is equal to m=0.9 (c.f. formula (42)). For each iteration k the error of numerical solution is calculated (c.f. equation (88))

$$E_k = \sqrt{\frac{1}{L^2}\sum_{l=1}^{L}\left[\nabla^2 U^{[1]}(x_l) - BU^{[1]}(x_l) + R\left[T_{k-1}(x_l, t^{f-1})\right]\right]_k^2} \tag{95}$$

If $E_k \leq 10^{-4}$ then the values $U^{[1]}(x_l)$ at the internal nodes x_l, $l = N$+1, ..., $N+L$ are accepted and the temperatures $T_k(x_l, t^f)$ (c.f. equation (42)) constitute the pseudo-initial condition for the next transition $t^f \rightarrow t^{f+1}$.

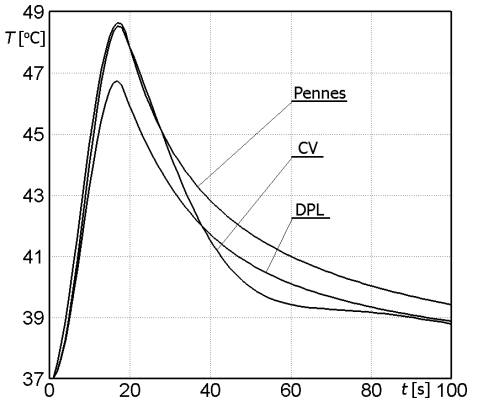

Figure 14: Temperature history at the point A

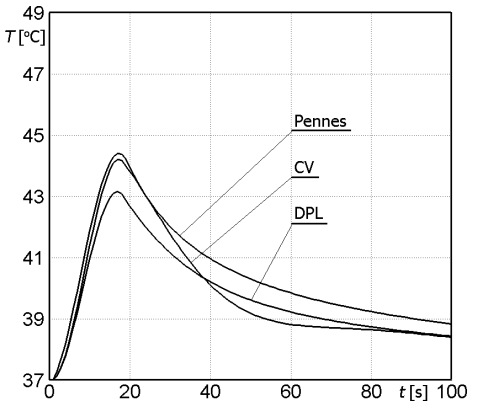

Figure 15: Temperature history at the point B

Figures 14 and 15 illustrate temperature history at the points A and B marked in Figure 13 for the Pennes, Catanneo-Vernotte (CV) and the DPL equations. The

differences between these solutions are visible, and in the case of DPL equation the temperatures are smaller in comparison with the Pennes or Cattaneo-Vernotte ones.

This example shows how important is proper choice of the model describing heat conduction in the tissue. For example, during the hyperthermia treatment the temperature in sub-domain considered should achieve 42-45°C, and if this procedure is simulated, the accuracy of temperature prediction is extremely important.

6 Conclusions

Different variants of the boundary element method for solving the bioheat transfer equations have been presented. For the steady state problems the multiple reciprocity boundary element method has been applied, while for transient bioheat transfer the 1^{st} scheme of the BEM, the BEM using discretization and the generalized boundary element method have been presented. The examples of computations show that the BEM is an effective tool for solving the different problems in the field of bioheat transfer.

It should be noted that the BEM was also used for numerical modeling of cryosurgery procedures [18, 33], the electric field effects in domain of biological tissue [34, 35], the laser-tissue interaction with tissue domain [36] and for identification of tumor position [14]. Recently the papers concerning the application of interval boundary element method [37, 38] appear. The problems considered concern, among others, the bioheat transfer ones [39].

Acknowledgement

The article and research were financed within the project NR13 0124 10 sponsored by Polish National Centre for Research and Development.

References

1. Huang, H.-W., Chan, C.-L., Roemer, R.-B. (1994) Analytical solutions of Pennes bio-heat transfer equation with a blood vessel. *Journal of Biomechanical Engineering*. 116, 208-212.

2. Pennes, H.-H. (1948) Analysis of tissue and arterial blood temperatures in the resting human forearm. *Journal of Applied Physiology.* 1, 93-122.

3. Cattaneo, C. (1958) A form of heat conduction equation which eliminates the paradox of instantaneous propagation. *Comp. Rend.* 247, 431-433.

4. Vernotte, P. (1948) Les paradoxes de la theorie continue de l'equation de la chaleur. *Comp. Rend.* 246, 3154-3155.

5. Xu, F., Seffen, K.-A., Lu, T.-J. (2008) Non-Fourier analysis of skin biothermomechanics. *International Journal of Heat and Mass Transfer*. 51, 2237-2259.

6. Zhou, J., Chen, J.-K., Zhang, Y. (2009) Dual-phase lag effects on thermal damage to biological tissues caused by laser irradiation. *Computers in Biology and Medicine.* 39, 286-293.

7. Brebbia, C.-A., Telles, J.C.-F., Wrobel, L.-C. (1984) *Boundary element techniques*, Springer-Verlag, Berlin, New York.

8. Banerjee, P.-K. (1994) *Boundary element methods in engineering*, McGraw-Hill Company, London.

9. Majchrzak, E. (2001) *Boundary element method in heat transfer*, Publication of the Czestochowa University of Technology, Czestochowa, 2001 (in Polish).

10. Nowak, A.-J., Brebbia, C.-A. (1989) The multiple reciprocity method - a new approach for transforming BEM domain integrals to the boundary. *Engineering Analysis with Boundary Elements*. 6(3), 164-167.

11. Curan, D.A.-S., Cross, M., Lewis, B.-A. (1980) Solution of parabolic differential equations by the boundary element method using discretisation in time. *Appl. Math. Modelling*. 4, 398-400.

12. Liao, S. (1997) General boundary element method for non-linear heat transfer problems governed by hyperbolic heat conduction equation. *Computational Mechanics*. 20, 397-406.

13. Majchrzak, E. (2010) Numerical solution of dual phase lag model of bioheat transfer using the general boundary element method. *CMES: Computer Modeling in Engineering and Sciences.* 69(1), 43-60.

14. Paruch, M., Majchrzak, E. (2007) Identification of tumor region parameters using evolutionary algorithm and multiple reciprocity boundary element method. *Engineering Applications of Artificial Intelligence.* 20, 647-655.

15. Ptaszny, J., Fedeliński, P. (2007) Fast multipole boundary element method for the analysis of plates with many holes. *Archives of Mechanics.* 59(4-5), 385-401.

16. Brebbia, C.-A., Nowak, A.-J. (1992) Solving heat transfer problems by the dual reciprocity BEM. *Boundary Element Method for Heat Transfer, Chapter*

1, Comp. Mech. Publications and Elsevier Applied Science, Southampton, 1-32..

17. Majchrzak, E. (1998) Numerical modelling of bio-heat transfer using the boundary element method. *Journal of Theoretical and Applied Mechanics*. 2(35), 437-455.

18. Majchrzak, E., Dziewoński, M. (2000) Numerical simulation of freezing process using the BEM. *Computer Assisted Mechanics and Engineering Sciences*. 7, 667-676.

19. Majchrzak, E., Jasiński, M. (2003) Numerical estimation of burn degree of skin tissue using the sensitivity analysis methods. *Acta of Bioengineering and Biomechanics*. 5(1), 93-108.

20. Majchrzak, E., Kałuża, G. (2006) Sensitivity analysis of biological tissue freezing process with respect to the radius of spherical cryoprobe. *Journal of Theoretical and Applied Mechanics*. 44(2), 381-392.

21. Liu, J., Xu, L.-X. (2000) Boundary information based diagnostics on the thermal states of biological bodies. *Journal of Heat and Mass Transfer*. 43, 2827-2839.

22. Zhou, J., Zhang, Y., Chen, J.-K. (2008) A dual reciprocity boundary element method for photothermal interactions in laser-induced thermotherapy. *International Journal of Heat and Mass Transfer*. 51, 3869-3881.

23. Drozdek, J., Majchrzak, E. (2007) Numerical solution of bioheat transfer equation by means of the dual reciprocity method. *Scientific Research of the Institute of Mathematics and Computer Science,* Czestochowa University of Technology, Czestochowa.1(6), 47-56.

24. Sladek, J., Sladek, V., Atluri, S.-N. (2004) Meshless local Petrov-Galerkin method for heat conduction problem in an anisotropic medium. *CMES: Computer Modeling in Engineering & Sciences*. 2(3), 309-318.

25. Liao, S., Chwang, A. (1999) General boundary element method for unsteady nonlinear heat transfer problems. *Numerical Heat Transfer*, Part B, 35, 225-242.

26. Romero, Mendez, R., Jimenez-Lozano, J.-N., Sen, M., Gonzalez, F.-J. (2010) Analytical solution of a Pennes equation for burn-depth determination from infrared thermographs. *Mathematical Medicine and Biology*. 27, 21-38, doi: 10.1093/imammb/dqp010.

27. Rumiński, J., Kaczmarek, M., Renkielska, A., Nowakowski, A. (2007) Thermal Parametric Imaging in the Evaluation of skin burn depth. *IEEE Transactions Biomedical Engineerning*. 54(2), 303-312.

28. Majchrzak, E. (2012) Determination of burn depth on the basis of skin surface temperature – solution of inverse problem using the gradient method. 10^{th} *World Congress on Computational Mechanics*, Sao Paulo, Brasil, CD ROM Proceedings, 12 pages.

29. Brinck, H., Werner, J. (1994) Estimation of the thermal effect of blood flow in a branching countercurrent network using a three dimensional vascular model. *Journal of Biomechanical Engineering.* 116, 324-330.

30. Majchrzak, E., Mochnacki, B. (1999) Numerical model of heat transfer between blood vessel and biological tissue. *Computer Assisted Mechanics and Engineering Sciences.* 6, 439-447.

31. Majchrzak, E., Tarasek, D. (2011) Numerical analysis of heat transfer in countercurrent blood flow and biological tissue. *Scientific Research of the Institute of Mathematics and Computer Science*, Czestochowa University of Technology, 2(10), 143-154.

32. Ferrera, M.-S., Yanagihara, J.-I. (2012) A heat transfer model of the human upper limbs. *International Communications in Heat and Mass Transfer*. 39, 196-203.

33. Majchrzak, E., Mochnacki, B., Dziewoński, M., Jasiński, M. (2011) Numerical modelling of hyperthermia and hypothermia processes. *Advanced Materials Research*. 268-270, 257-262.

34. Majchrzak, E., Dziatkiewicz, G., Paruch, M. (2008) The modelling of heating a tissue subjected to external electromagnetic field. *Acta of Bioengineering and Biomechanics*. 10(2), 29-37.

35. Majchrzak, E., Paruch, M. (2011) Identification of electromagnetic field parameters assuring the cancer destruction during hyperthermia treatment. *Inverse Problems in Science & Engineering*. 19(1), pp. 45-58.

36. Jasiński, M. (2009) Sensitivity Analysis Of Bioheat Transfer In Human Cornea Subjected To Laser Irradiation. Part 1: Variation Of Optical Parameters, *Scientific Research of the Institute of Mathematics and Computer Science*, Czestochowa University of Technology, 8(1), 63-70.

37. Piasecka-Belkhayat, A. (2011) Interval boundary element method for 2D transient diffusion problem using the directed interval arithmetic. *Engineering Analysis with Boundary Elements*. 35(3), 259-263.

38. Piasecka-Belkhayat, A. (2011) Interval boundary element method for transient diffusion problem in two-layered domain. *Journal of Theoretical and Applied Mechanics*. 49(1), 267-276.

39. Piasecka-Belkhayat, A., Jasiński, M. (2011) Modelling of UV laser irradiation of anterior part of human eye with interval optic parameters. *Evolutionary and Deterministic Methods for Design, Optimization and Control. Applications to Industrial and Societal Problems* (Eds. T. Burczyński, J. Périaux), 316 -321, CIMNE, Barcelona.